nature cell biology

# Genetic control of single lumen formation in the zebrafish gut

Michel Bagnat[1,3], Isla D. Cheung[1], Keith E. Mostov[2] and Didier Y. R. Stainier[1,3]

**Most organs consist of networks of interconnected tubes that serve as conduits to transport fluid and cells and act as physiological barriers between compartments. Biological tubes are assembled through very diverse developmental processes that generate structures of different shapes and sizes. Nevertheless, all biological tubes invariably possess one single lumen. The mechanisms responsible for single lumen specification are not known. Here we show that zebrafish mutants for the MODY5 and familial GCKD gene *tcf2* (also known as *vhnf1*) fail to specify a single lumen in their gut tube and instead develop multiple lumens. We show that Tcf2 controls single lumen formation by regulating *claudin15* and $Na^+/K^+$-ATPase expression. Our *in vivo* and *in vitro* results indicate that Claudin15 functions in paracellular ion transport to specify single lumen formation. This work shows that single lumen formation is genetically controlled and appears to be driven by the accumulation of fluid.**

The zebrafish gut tube originates from a solid rod of endodermal cells that forms a lumen as the cells polarize, but without apoptosis[1–3]. Tcf2 has been shown to be required for endoderm differentiation in mammals[4], and zebrafish *tcf2* mutants have defects in gut, liver and pancreas morphogenesis[5]. To explore the role of *tcf2* in zebrafish gut tube formation we used the null insertional allele $tcf2^{2169}$ (ref. 5) and analysed gut morphology 72 h post fertilization (h.p.f.) by confocal microscopy. In transverse section, some $tcf2^{2169}$ mutants showed pronephric cysts, as reported previously[5]; most strikingly, however, some mutants presented multiple lumens in the intestinal bulb, the region of the zebrafish intestine that acts as a stomach (Fig. 1a, top). These phenotypes could be found together or separately and are therefore most probably independent from each other. Using a membrane-bound green fluorescent protein we observed lumens that were open through long stretches and also others that were only a few cells long (see Supplementary Information, Fig. S1). We did not observe multiple lumens in the posterior gut, a part of the tube that has fewer cells (not shown). To determine whether tight and adherens junctions were properly formed in $tcf2^{2169}$ mutant gut epithelial cells, we stained transverse sections with antibodies against cadherin and the tight junction marker zonula occludens protein-1 (ZO-1). At 72 h.p.f., about half of the mutant larvae (47.5%, $n = 101$) presented multiple gut lumens in which both markers were localized correctly. A fraction of the mutants (17.8%) did not show a discernible lumen and presented an unpolarized distribution of cadherin (Fig. 1a). In contrast, we could not find any multiple lumen gut in wild-type (WT) larvae at 72 h.p.f. ($n = 250$). To understand normal gut morphogenesis we examined WT embryos at different time points. At about 36 h.p.f., some cells of the endodermal rod expressed the junctional marker ZO-1 and showed some degree of polarization, but no obvious luminal structure could be observed. Then, at about 43 h.p.f., we observed multiple small lumens marked by ZO-1 (Fig. 1b), and apparent as small clear spaces by transmission electron microscopy (see Supplementary Information, Fig. S1). These multiple lumens coalesced into a single larger lumen by 48 h.p.f. (Fig. 1b). At 96 h.p.f., the multiple lumen phenotype was still present in $tcf2^{2169}$ mutants (Fig. 1a), suggesting that this phenotype represents an arrest in the lumen formation process. These data indicate that single lumen formation in the zebrafish intestinal bulb is a very efficient process that involves the coalescence of multiple small lumens and is controlled by the transcription factor Tcf2.

Next we analysed potential downstream effectors of Tcf2. The atypical protein kinase C λ (aPKC-λ, also known as prkci) mutant *heart and soul* (*has*) was previously shown to develop multiple lumens in the gut[6]. However, the penetrance of this phenotype is much lower in *has* (7.8%, $n = 152$) than in $tcf2^{2169}$ mutant larvae (see Supplementary Information, Fig. S2). In addition, aPKC-λ expression levels did not seem to be affected in $tcf2^{2169}$ mutants (see Supplementary Information, Fig. S2), suggesting that aPKC-λ is not an effector of Tcf2 in gut lumen formation. Because apical membrane formation has been implicated in tubulogenesis and lumen expansion in *Drosophila*[7], we tested whether apical membrane formation was affected in $tcf2^{2169}$ mutant larvae. We first examined the localization of aPKC-λ and the apical antigen 4e8 (ref. 8) and found that they were expressed and localized properly in

[1]Department of Biochemistry & Biophysics, Programs in Developmental Biology, Genetics and Human Genetics, University of California, San Francisco, 1550 Fourth Street, San Francisco, California 94158-2324, USA. [2]Department of Anatomy, University of California, San Francisco, 600 16th Street, San Francisco, California 94147-2140, USA.
[3]Correspondence should be addressed to M.B. (e-mail: michel.bagnat@ucsf.edu) or D.Y.R.S. (e-mail: dstainier@biochem.ucsf.edu)

Received 31 January 2007; accepted 22 June 2007; published online 15 July 2007; DOI: 10.1038/ncb1621

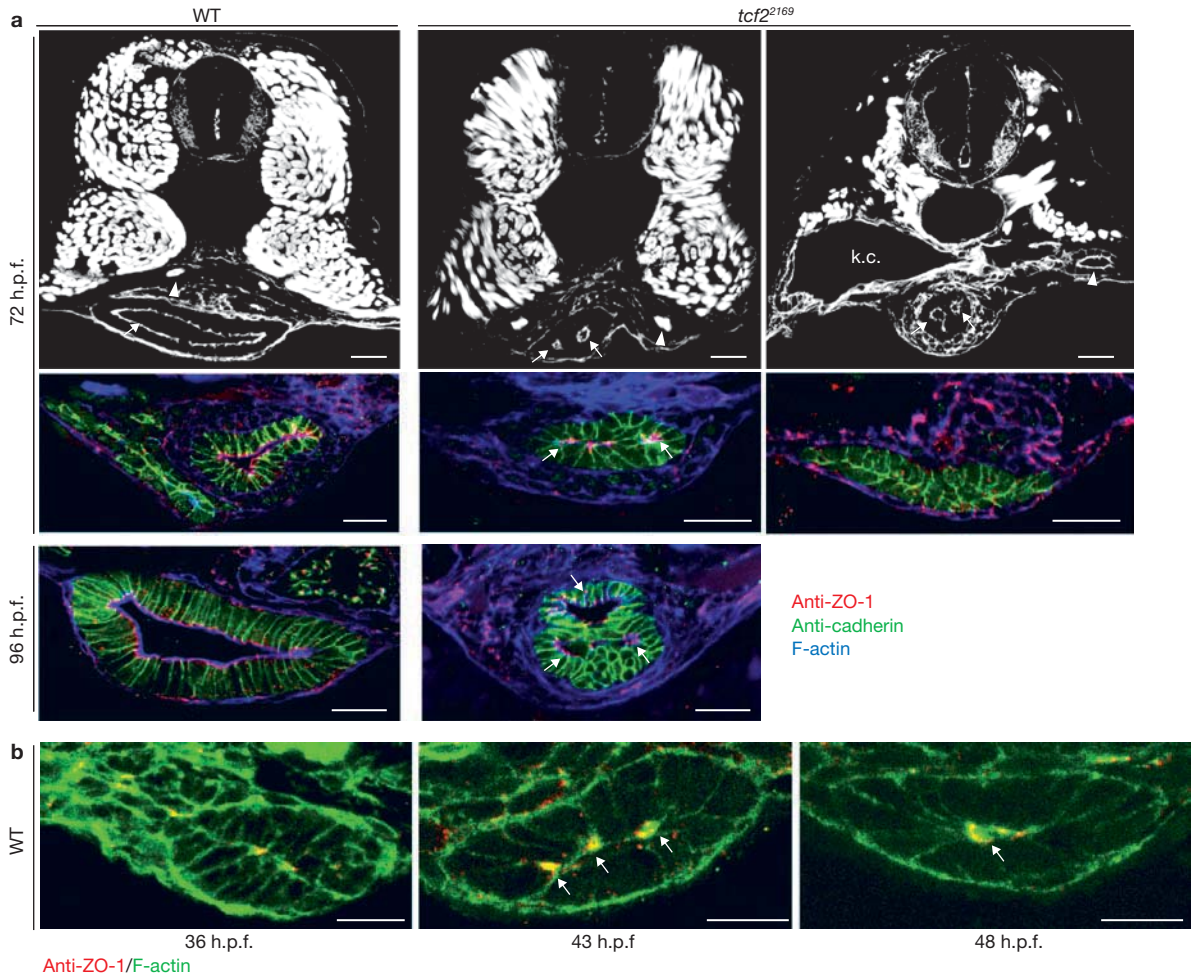


**Figure 1** Gut lumen formation in WT and *tcf2*$^{2169}$ mutant larvae. **a**, Top: confocal images of transverse sections of 72 h.p.f. WT and *tcf2*$^{2169}$ mutant larvae stained with rhodamine-phalloidin to visualize F-actin. Multiple lumens are present in the gut of *tcf2*$^{2169}$ mutant larvae at 72 h.p.f. The arrows point to the gut lumens and the arrowheads to the pronephric duct lumen. k.c., kidney cyst. Middle: confocal images of transverse sections of 72 h.p.f. WT and *tcf2*$^{2169}$ mutant larvae stained for pan-cadherin (green), ZO-1 (red) and alexa647-phalloidin (blue). Bottom: 96 h.p.f. WT and *tcf2*$^{2169}$ mutant larvae processed as in the middle panel. **b**, Confocal images of transverse sections of WT larvae collected at the indicated time points, stained for F-actin (green, false colour) and ZO-1 (red). At 43 h.p.f. multiple lumens can be seen (arrows). Scale bars, 20 μm.

*tcf2*$^{2169}$ mutant larvae (see Supplementary Information, Fig. S2). Next we examined two mutants that had previously been shown to be affected in different aspects of apical membrane biogenesis in the retinal epithelium. Both *mosaic eyes* (*moe*, also known as *epp41l5*)[9] and *naggie oko* (*nok*, also known as *mpp5*)[10] mutants showed small gut lumens but did not present a multiple lumen phenotype (see Supplementary Information, Fig. S2). These data suggest that apical membrane expansion does not have a major role in gut lumen coalescence.

To identify Tcf2-regulated factors involved in single lumen formation we used DNA microarray analyses to find genes downregulated in *tcf2*$^{2169}$ mutants compared with WT. Consistent with previous work[5] was our observation, among the genes regulated by Tcf2, of several enzyme-coding genes specific to liver and pancreas, including a liver fatty-acid-binding-protein gene (*lfabp10*) whose expression was decreased 20-fold. We confirmed these data by looking at the expression of DsRed driven by the *lfabp* promoter[11] (*lfabp:DsRed*) in WT and *tcf2*$^{2169}$ mutant larvae (Fig. 2a). When we examined genes that showed a more than twofold decrease in expression levels, we found that *claudin15* (*cldn15*) was downregulated 5.3-fold in *tcf2*$^{2169}$ mutants compared with WT (for a partial list of genes downregulated in *tcf2*$^{2169}$ mutant larvae see Supplementary Information, Table S1). To check whether *cldn15* expression is indeed regulated by Tcf2 we performed *in situ* hybridization (ISH) analysis. At 72 h.p.f., we could detect *cldn15* expression in the gut of WT but not *tcf2*$^{2169}$ mutant larvae (Fig. 2b). Next we examined *cldn15* expression during WT development. We detected expression in the midgut at about 36 h.p.f. that became stronger and extended towards the posterior gut later in development (Fig. 2c). At 72 h.p.f., *cldn15* expression could also be detected in the pronephros and pancreas. These data show that *cldn15* is expressed in the gut under the control of Tcf2 at the time when lumen coalescence takes place.

To test whether Cldn15 is required for single lumen formation we knocked down its expression by using a morpholino directed against the translation initiation site. Most (more than 80%) Cldn15 morphants phenocopied *tcf2*$^{2169}$ mutants (Fig. 2d). When we analysed gut lumen formation in Cldn15 morphants, we found that a significant fraction (34.7%, $n = 78$) showed a multiple lumen phenotype in the intestinal bulb that did not affect the localization of cadherin or ZO-1 (Fig. 2e). The phenotype of Cldn15 morphants was specific to the gut, because

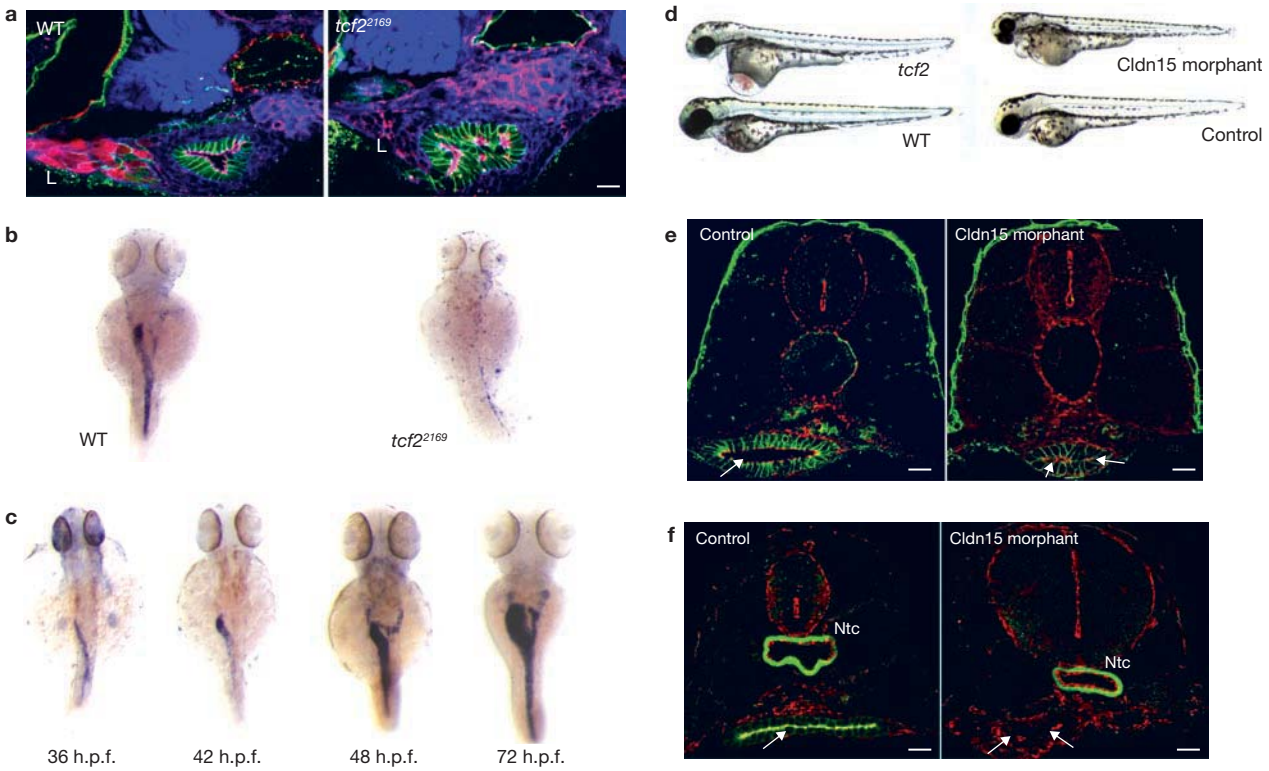


**Figure 2** Tcf2 controls Cldn15 expression in the gut; Cldn15 knockdown larvae have multiple gut lumens. **a**, lfabp:DsRed is expressed at 72 h.p.f. in the liver (L) of WT larvae but undetectable in *tcf2*$^{2169}$ mutant larvae. Larvae were fixed, sectioned and stained for cadherin (green), ZO-1 (red) and F-actin (blue). Scale bar, 20 μm. **b**, *cldn15 in situ* hybridization. *cldn15* is expressed in the gut of WT larvae but not in that of *tcf2*$^{2169}$ mutant larvae at 72 h.p.f. **c**, Time course of *cldn15* expression in WT larvae. **d**, Whole-body phenotype of *tcf2*$^{2169}$ mutant larvae and Cldn15 morphants at 72 h.p.f. **e**, Confocal images of transverse sections of control (uninjected) larvae and Cldn15 morphants stained for cadherin (green) and ZO-1 (red). Arrows points to the gut lumens. **f**, Cldn15 (green) colocalizes with ZO-1 (red) at the tight junction in WT larvae. Expression of Cldn15 is abolished in the morphants. The antibody used for Cldn15 also reacts with an antigen expressed in the notochord (Ntc). Scale bars, 20 μm.

the pronephric and neural tubes were not affected (Fig. 2e). To confirm that Cldn15 was indeed knocked down we analysed Cldn15 expression and localization by using an antibody generated against human Cldn10, a protein that shares significant homology to zebrafish Cldn15 (ref. 12). This antibody specifically recognized zebrafish Cldn15 transfected into HEK293 cells (see Supplementary Information, Fig. S3), a human cell line that does not express claudins. In WT zebrafish larvae, this antibody stained tight junctions in the gut and pronephros, where it colocalized with ZO-1. It also stained the notochord where colocalization with ZO-1 was only partial (Fig. 2f). The notochord signal most probably corresponds to another antigen, perhaps another claudin, that crossreacts with the antibody, because we did not detect *cldn15* expression in the notochord. Importantly, the staining was absent in the gut of Cldn15 morphants (Fig. 2f), indicating that Cldn15 was effectively knocked down by the morpholino. The multiple lumen phenotype observed in Cldn15 morphants seems to be specific because larvae in which the tight-junction protein occludin was knocked down did not show any defects in gut lumen formation ($n = 35$) (see Supplementary Information, Fig. S3). Taken together, these data strongly suggest that Tcf2 controls lumen coalescence in the zebrafish gut, at least in part through Cldn15.

Recently, the *Drosophila* claudin mutants *sinuous*[13] and *megatrachea*[14] were shown to have tracheal tube defects. In both mutants, assembly of the septate junction—the functional equivalent of the vertebrate tight junction—and the barrier function in tracheal epithelial cells was affected. To test whether the barrier function was compromised in *tcf2*$^{2169}$ mutants, we injected the yolk of 72 h.p.f. WT and mutant larvae with two tracers that had been previously used to assay the barrier function in vertebrates, rhodamine-dextran of relative molecular mass 10,000 ($M_r$ 10K) and a biotinylation reagent ($M_r$ 443)[15], to determine whether they reached the apical side of gut epithelial cells. In WT and *tcf2*$^{2169}$ mutant larvae, both tracers reached the basolateral surface of gut epithelial cells and marked the entire lateral surface but could not be detected on the apical side (Fig. 3a). This experiment, together with the normal localization of ZO-1, indicates that in *tcf2*$^{2169}$ mutants the tight junctions in the gut are still present and able to function as barriers for molecules of $M_r$ 443 or more, probably as a result of the presence of other claudins that are not regulated by Tcf2 (data not shown).

Claudins have also been shown to form paracellular pores that allow the selective passage of ions across epithelia down an electrochemical gradient formed by the $Na^+/K^+$-ATPase[16,17]. Mutations in *CLDN16* cause familial hypomagnesaemia in humans[18]. When transfected into LLC-PK1 epithelial cells, CLDN16 increases paracellular permeability to $Na^+$, suggesting that the lack of $Mg^{2+}$ reabsorption probably resulted from a dissipation of the transepithelial potential[19]. Paracellular ion permeability can be estimated by measuring the transepithelial electrical resistance (TER). TER is high in 'tight' epithelia and low in 'leaky' epithelia[17,20,21]. Expression of different claudins in various cell lines can either increase or decrease their TER; this measure has therefore been used to determine the ion pore-forming properties of claudins[20,22]. We hypothesized that Cldn15 might form a paracellular pore that would allow the movement of ions

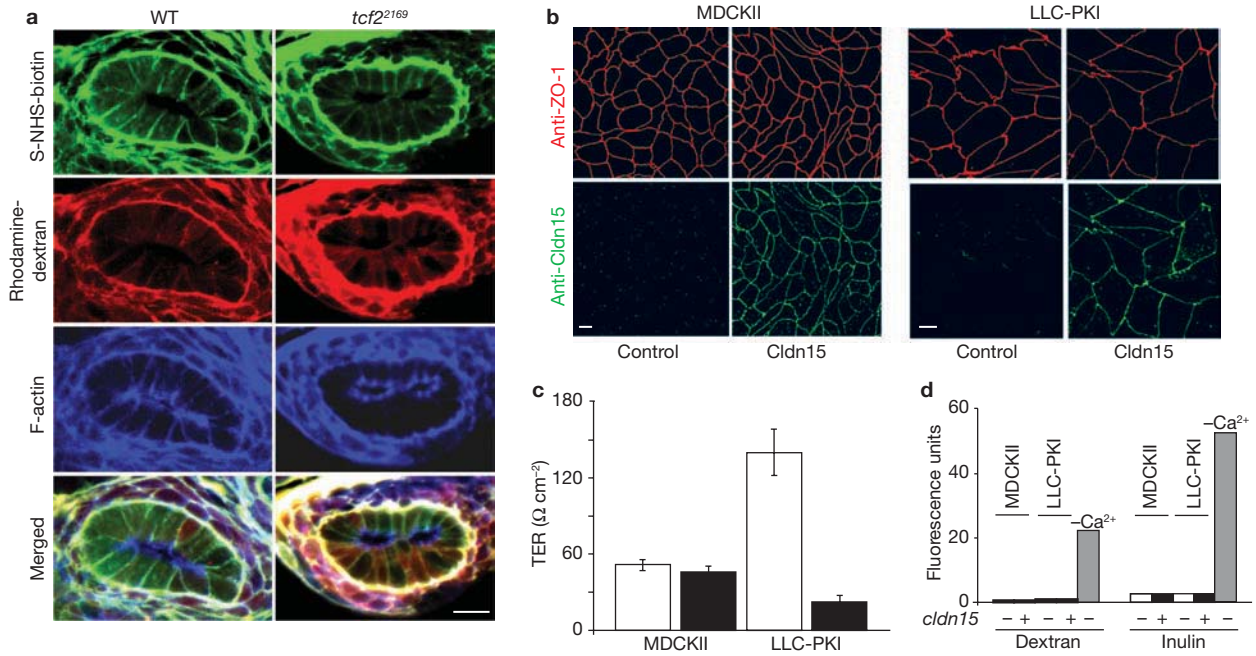


**Figure 3** Cldn15 forms a paracellular ion pore. **a**, The epithelial barrier remains functional in *tcf2*$^{2169}$ mutant larvae. Rhodamine-dextran ($M_r$ 10K) and the biotinylation reagent sulpho-NHS-biotin (S-NHS-biotin) were injected into the yolk of 72 h.p.f. WT and *tcf2*$^{2169}$ mutant larvae. After 2 h, larvae were fixed and the distribution of the tracers was examined by confocal microscopy. Green, S-NHS-biotin; red, rhodamine-dextran; blue, F-actin. Scale bar, 20 μm. **b**, Cldn15 (green) colocalizes with ZO-1 (red) in cell lines stably expressing Cldn15. Scale bar, 10 μm. **c**, Stable Cldn15 expression (filled bars) reduces the TER in LLC-PK1 cells but not in MDCKII cells ($n = 6$) compared with control cells (open bars), which were transfected with an empty vector. Similar results were obtained with two independent clones for each cell line (only one is shown for each). Error bars indicate s.d. **d**, Epithelial sheets retained barrier function. Diffusion of fluorescent tracers (rhodamine-dextran ($M_r$ 10K) and FITC-inulin) was not affected by the expression of Cldn15. Cells incubated in buffer without $Ca^{2+}$, a treatment used to open the junctions, were used as a reference.

and fluid into the gut lumen; in turn, fluid accumulation would provide the force to drive lumen coalescence. To test this hypothesis, we generated cell lines stably expressing untagged Cldn15. When expressed in MDCKII or LLC-PK1 cells, Cldn15 was efficiently targeted to the tight junction and colocalized with ZO-1 (Fig. 3b). Although Cldn15 expression in the low TER MDCKII background did not change the TER significantly ($n = 6$), it markedly decreased (sevenfold, $n = 6$) the TER in tighter LLC-PK1 cells compared with control cells (transfected with empty vector) (Fig. 3c), indicating that Cldn15 can form ion-permeable pores in epithelial tight junctions. Importantly, even though the TER was reduced, the epithelial sheet remained tight and did not allow transepithelial passage of two different tracers, $M_r$ 10K rhodamine-dextran and fluorescein isothiocyanate (FITC)-inulin ($M_r$ 2K–5K) (Fig. 3d).

To test the role of fluid accumulation, as well as of Cldn15, during lumen formation, we optimized an *in vitro* lumen formation assay by using epithelial cysts cultured over a thin layer of Matrigel. We initially used the LLC-PK1 cell lines that we generated; however, these cells did not form cysts (data not shown). To circumvent this limitation we turned to MDCKC7 cells, which display a very high TER[23]. Stable lines expressing Cldn15 (Fig. 4a) showed a very drastic decrease in TER compared with control cells (Fig. 4b), confirming the results obtained with LLC-PK1 cells. We next cultured these cells in Matrigel to assess the effect of Cldn15 on lumen formation. After 4 days in culture, control MDCKC7 cells formed single lumen cysts, somewhat inefficiently (only 44% single lumen), that were mostly (92%) smaller than 50 μm in lumen diameter; only 8% had a lumen that was 50–100 μm wide. On expression of Cldn15, the fraction of cysts with a single lumen increased by more than 60% ($P = 0.0002$). This effect was accompanied by a significant increase in lumen size, with a large fraction of cysts (49.3%) having a lumen 50–100 μm wide and a significant fraction (12.7%) being larger than 100 μm (Fig. 4d, left panels). Next, to test the role of fluid accumulation on single lumen formation we treated cysts with forskolin and/or ouabain. Forskolin has been shown to promote fluid accumulation and cyst lumen expansion, mainly through the kinase-dependent activation of apical chloride channels[24,25]. In contrast, inhibition of the $Na^+/K^+$-ATPase with the glycoside ouabain disrupts the formation of the electrochemical gradient necessary to drive paracellular and transcellular ion transport, thus producing the opposite effect (a diagram is shown in Fig. 4c). The addition of forskolin (10 μM) not only led to a marked increase in cyst lumen size as shown before with other cell types[25], but also increased by more than 50% the fraction of MDCKC7 cysts with a single lumen ($P = 0.0095$). Forskolin was significantly more effective in cells expressing Cldn15 ($P = 0.022$ compared with MDCKC7 plus forskolin; $P = 0.0065$ compared with Cldn15 control), indicating a synergy between paracellular and transcellular ion transport. Conversely, ouabain (0.1 μM) blocked single lumen formation and expansion (all lumens were smaller than 50 μm) in all cases (Fig. 4c). These data show a direct role for Cldn15 in single lumen formation and lumen size control, and they illustrate the role of fluid accumulation in this process *in vitro*. To investigate whether this mechanism also operates *in vivo*, we injected the yolk of 30 h.p.f. WT embryos with small amounts of ouabain or forskolin and analysed lumen formation in the gut as before. Injection of forskolin led to a significant enlargment of the gut lumen. In contrast, injection of ouabain produced a dose-dependent multiple lumen

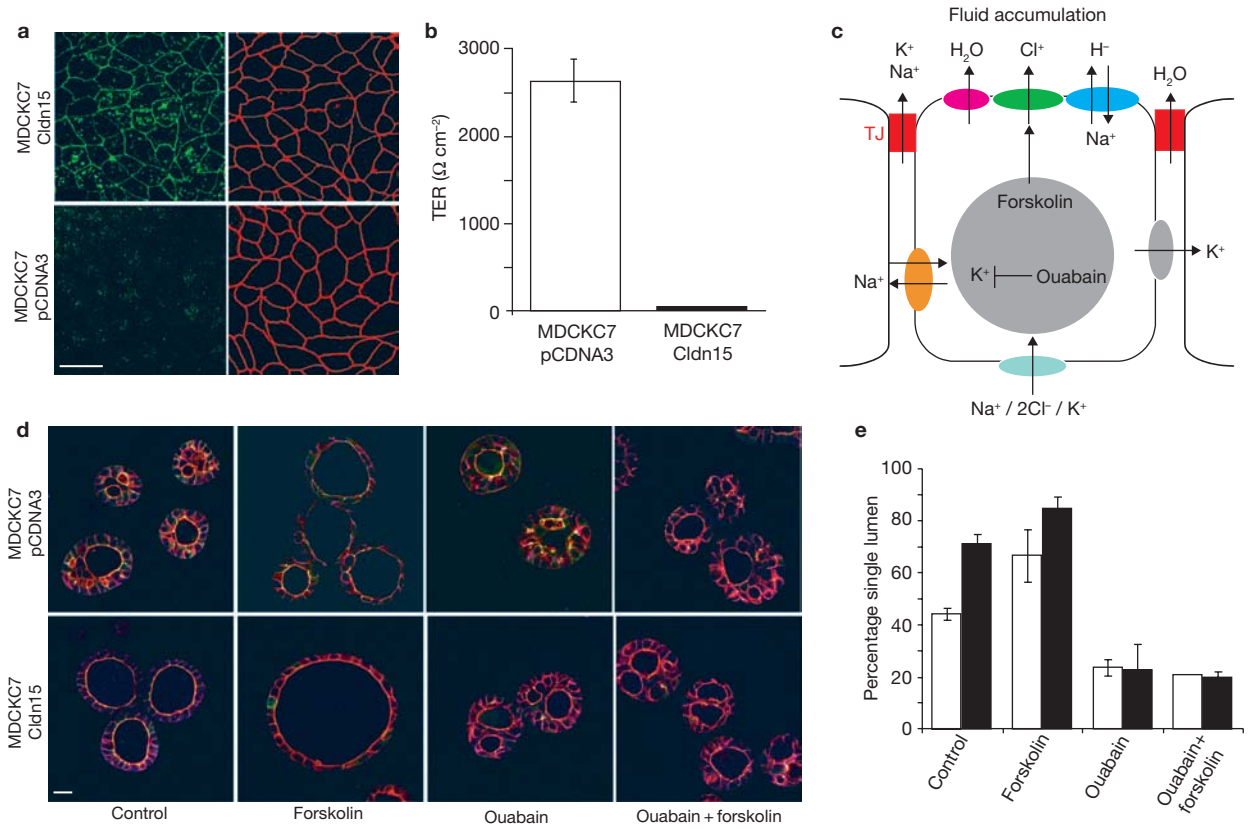


**Figure 4** Cldn15 promotes single lumen formation through a fluid-driven mechanism. **a**, Cldn15 (green) colocalizes with ZO-1 (red) in MDCKC7 cells stably expressing Cldn15. Scale bar, 10 μm. **b**, Stable Cldn15 expression reduces the TER in MDCKC7 cells compared with that in control cells, which were transfected with an empty vector ($n = 4$). Diffusion of fluorescent tracers (rhodamine-dextran ($M_r$ 10K) and FITC-inulin) was not affected by the expression of Cldn15 (not shown). **c**, Simplified scheme of ion and water transport through the transcellular and paracellular routes. Forskolin activates apical chloride secretion and fluid accumulation, whereas ouabain inhibits the $Na^+/K^+$-ATPase and disrupts electrochemical gradient formation. TJ, tight junction. **d**, Lumen formation in cysts. Control MDCKC7 cells or Cldn15-expressing cells were grown for 2 days over a thin layer of Matrigel to allow cyst formation. The medium was then replaced with fresh medium containing DMSO (control), forskolin (10 μM) or ouabain (0.1 μM) and cells were cultured for a further 2 days. Cysts were stained for F-actin (red), ZO-1 (green) and β-catenin (blue) and examined by confocal microscopy. Scale bar, 20 μm. **e**, Quantification of three independent experiments shown in **d**. Filled bars, Cldn15-expressing cells; open bars, control cells. Error bars indicate s.d. (from left to right, $n = 312$, 325, 351, 327, 305, 310, 321 and 338).

phenotype (26% multiple lumen ($n = 46$) with 3 nl of 100 μM ouabain; 50% ($n = 26$) with 3 nl of 200 μM ouabain) that was identical to that in *tcf2*$^{2169}$ mutant larvae (Fig. 5a). We next tried to rescue *tcf2*$^{2169}$ mutants by injecting forskolin. Because forskolin had no effect on *tcf2*$^{2169}$ mutants (Fig. 5a), we checked expression of the $Na^+/K^+$-ATPase. Staining with antibodies revealed that although the protein was expressed at wild-type or higher levels in the pronephros and neural tube it was absent from the gut of *tcf2*$^{2169}$ mutants, indicating that Tcf2 also controls $Na^+/K^+$-ATPase expression in the gut (Fig. 5b).

Here we have shown that the formation of a single lumen, a defining characteristic of all biological tubes, is genetically controlled. Our data demonstrate that regulation of Cldn15 and $Na^+/K^+$-ATPase expression by Tcf2 is required for single lumen specification in the intestinal bulb of the zebrafish gut. The posterior gut and pronephros, which also express Cldn15 under the control of Tcf2, did not show defects in lumen formation. This difference can be explained by the fact that in these tubes all cells are in close proximity and are therefore able to establish continuous tight junctions before the lumen opens.

Claudins have been shown to form $Ca^{2+}$-independent adhesions when transfected into fibroblasts, through the interaction of the extracellular domains of molecules present in adjacent cells[26]. We were able to recreate this phenomenon in HEK293 cells expressing zebrafish Cldn15 (see Supplementary Information, Fig. S3). However, although it is possible that claudin-based cell–cell adhesion may contribute to the process, it is unlikely that protein–protein interactions alone would be able to drive the coalescence of lumens that may be several cells apart. We propose that the electrochemical gradient generated by the $Na^+/K^+$-ATPase drives vectorial ion movement through Cldn15-based paracellular pores. Asymmetric ion distribution would produce luminal fluid accumulation that would lead to the expansion of multiple small lumens and provide the force for their coalescence (Fig. 5c).

To maintain an open luminal space, all biological tubes must be filled with liquid, gas or other materials at all times. Recent work in *Drosophila* has revealed a role for apical matrix deposition during lumen formation in the retina[27] and tracheal system[28,29]. In both cases it seems that the apical matrix functions as a scaffold to support the initial stages of lumen formation. In vertebrates, fluid accumulation has been implicated in neural tube expansion[30]. Our work suggests that fluid accumulation could simultaneously provide the driving force for lumen expansion and ensure that a single lumen is formed. □

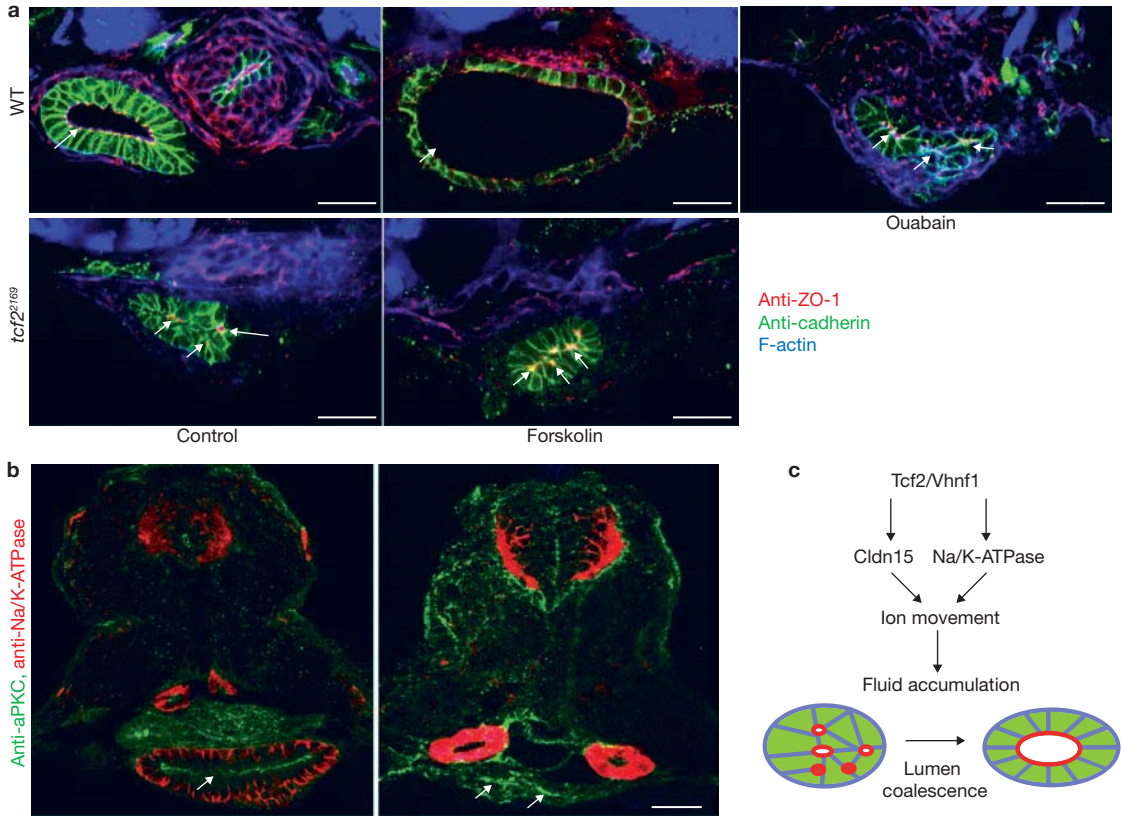


**Figure 5** Disruption of the $Na^+/K^+$-ATPase-dependent electrochemical gradient blocks lumen coalescence. **a,** Top: confocal images of transverse sections of 72 h.p.f. WT larvae injected at 30 h.p.f. in yolk with 3 nl of ouabain (200 μM) or forskolin (10 μM) stained for pan-cadherin (green), ZO-1 (red) and Alexa647-phalloidin (blue). Bottom: *tcf2*$^{2169}$ mutant larvae injected with DMSO (control) or forskolin as indicated above. The arrows point to the gut lumen. Scale bars, 20 μm. **b**, Tcf2 controls expression of the $Na^+/K^+$-ATPase in the zebrafish gut. $Na^+/K^+$-ATPase is shown in red and aPKC in green. Scale bar, 20 μm. **c,** Diagram of Tcf2-controlled lumen coalescence.

## METHODS

**Animals.** AB wild-type and mutant alleles *tcf2*$^{2169}$, *has*$^{m567}$, *moe*$^{b781}$ and *nok*$^{m520}$ were maintained as described previously[11,15,18,19]. The *tcf2*$^{2169}$ mutation was crossed into the *lfabp:DsRed* transgenic line[31].

**Cells and antibodies.** MDCKII cells were grown in MEM medium supplemented with 5% fetal bovine serum. LLC-PKI cells were grown in M-199 medium supplemented with 3% fetal bovine serum. HEK293 cells were grown in DMEM medium supplemented with 10% fetal bovine serum. Antibodies against human ZO-1, Cldn10 and occludin were from Zymed (Carlsbad, CA, USA). Rabbit anti-pan-cadherin was from Sigma, and rabbit anti-aPKC was from Santa Cruz (Santa Cruz, CA, USA). Mouse monoclonal antibody 4e8 (ref. 17) was provided by J. Lewis (Cancer ResearchUK London Institute, London, UK). Alexa647-phalloidin was from Molecular Probes.

**Expression vectors and stable cell lines.** To establish stable cell lines expressing zebrafish Cldn15 (accession number NM_200404) the full-length cDNA was amplified by PCR from a full-length cDNA clone (catalogue number 6791205; Open Biosystems, Huntsville, AL, USA) and inserted into the mammalian expression vector pCDNA3 (Invitrogen, Carlsbad, CA, USA). Cells were transfected with Lipofectamine 2000 (Promega, Madison, WI, USA). MDCKII and LLC-PKI cells expressing Cldn15 were selected in medium containing 500 and 750 μm $ml^{-1}$ G418, respectively.

**Morpholino knockdown.** The Cldn15 (MORPH1234, 5′-ATGATCGGATCC ATTGTAGCTGCAG-3′; Open Biosystems) and occludin a (MORPH1463, 5′-GACTCCCGATGTGCTTCGACGACA-3′; Open Biosystems) morpholinos were targeted against the translational start.

***In situ* hybridization.** Whole-mount *in situ* hybridizations were performed as described previously[8]. The *clnd15* (accession number NM_200404) *in situ* probe corresponds to nucleotides 589–1158. The *in situ* construct was cloned into pGEMT-easy (Promega) with *Bam* HI/*Xho* I, linearized with *Xho* I and transcribed with T7 RNA polymerase.

**Immunohistochemistry.** For pan-cadherin and F-actin staining, larvae were fixed in 4% formaldehyde in egg water at 4 °C overnight. The fixed larvae were washed in PBS and embedded in 4% low-melt agarose in PBS. Transverse sections 250 μm thick were obtained with a vibratome (Leica, Bannockburn, IL, USA). For Cldn15 and occludin stainings, larvae were fixed in trichloroacetic acid for 1 h on ice.

**Immunofluorescence.** After 7 days of culture on transwell filters, cells were fixed with 10% trichloroacetic acid and stained as described previously[6].

**Confocal imaging.** Confocal imaging was performed with a Zeiss LSM510 laser-scaning microscope. Images were analysed with LSM software (Zeiss, Thornwood, NY, USA) and Photoshop 7.0 (Adobe).

***In vivo* paracellular tracer flux assay.** Larvae at 72 h.p.f. were anaesthetized in 0.1 mg $ml^{-1}$ tricaine (Sigma, St Louis, MO, USA) and injected into the yolk with 10–20 nl of 1% rhodamine-dextran ($M_r$ 10K; Molecular Probes, Carlsbad, CA, USA) and 10 mg $ml^{-1}$ EZ-Link sulpho-NHS-biotin (Pierce, Rockford, IL, USA) in 0.2 M KCl. After incubation for 2 h at 28 °C, larvae were fixed and processed for immunohistochemistry. Biotin was detected with Alexa488-streptavidin.

**Measurement of TER and paracellular tracer flux.** After 7 days of culture on transwell filters, TER was measured directly in culture medium at 24 °C with a

Millicell-ERS epithelial voltohmmeter (Millipore, Billerica, MA, USA).

Paracellular tracer flux was measured with 1 mg $ml^{-1}$ rhodamine-dextran ($M_r$10K) and FITC-inulin (Sigma) as described previously[6].

**Lumen formation in epithelial cysts.** Control MDCKC7 and Cldn15-expressing cells were grown on DMEM (H21) medium supplemented with 2% Matrigel over a thin layer of 100% Matrigel for 2 days, to allow cyst formation. Then the medium was replaced with fresh medium containing 2% Matrigel and dimethylsulphoxide (DMSO; control), forskolin (10 μM) or ouabain (0.1 μM) and cells were cultured for a further 2 days.

**Gene accession numbers.** *lfabp10* (NM_152960), *cldn15* (NM_200404), *occludin a* (NM_21832).

*Note: Supplementary Information is available on the Nature Cell Biology website.*

ACKNOWLEDGEMENTS

We thank S. Huling and the UCSF liver centre for electron microscopy; C. Van Itallie, J. M. Anderson and H. Oberleithner for providing cell lines; F. M. Belmonte, L. Katz and V. Bhalla for advice on the *in vitro* experiments; and K. Simons, T. Mikawa, F. M. Belmonte and C. Eroglu for critically reading the manuscript. M.B. was supported by an EMBO long-term fellowship. This work was supported in part by grants from the Packard Foundation and the NIH to D.Y.R.S.

COMPETING FINANCIAL INTERESTS

The authors declare no competing financial interests.

Published online at http://www.nature.com/naturecellbiology/
Reprints and permissions information is available online at http://npg.nature.com/reprintsandpermissions/

1. Ober, E. A., Field, H. A. & Stainier, D. Y. From endoderm formation to liver and pancreas development in zebrafish. *Mech. Dev.* **120,** 5–18 (2003).
2. Ng, A. N. *et al.* Formation of the digestive system in zebrafish. III. Intestinal epithelium morphogenesis. *Dev. Biol.* **286,** 114–135 (2005).
3. Wallace, K. N. & Pack, M. Unique and conserved aspects of gut development in zebrafish. *Dev. Biol.* **255,** 12–29 (2003).
4. Barbacci, E. *et al.* Variant hepatocyte nuclear factor 1 is required for visceral endoderm specification. *Development* **126,** 4795–4805 (1999).
5. Sun, Z. & Hopkins, N. *vhnf1*, the MODY5 and familial GCKD-associated gene, regulates regional specification of the zebrafish gut, pronephros, and hindbrain. *Genes Dev.* **15,** 3217–3229 (2001).
6. Horne-Badovinac, S. *et al.* Positional cloning of heart and soul reveals multiple roles for PKC λ in zebrafish organogenesis. *Curr. Biol.* **11,** 1492–1502 (2001).
7. Lubarsky, B. & Krasnow, M. A. Tube morphogenesis: making and shaping biological tubes. *Cell* **112,** 19–28 (2003).
8. Crosnier, C. *et al.* Delta–Notch signalling controls commitment to a secretory fate in the zebrafish intestine. *Development* **132,** 1093–1104 (2005).
9. Jensen, A. M. & Westerfield, M. Zebrafish mosaic eyes is a novel FERM protein required for retinal lamination and retinal pigmented epithelial tight junction formation. *Curr. Biol.* **14,** 711–717 (2004).
10. Wei, X. & Malicki, J. *nagie oko*, encoding a MAGUK-family protein, is essential for cellular patterning of the retina. *Nature Genet.* **31,** 150–157 (2002).
11. Her, G. M., Yeh, Y. H. & Wu, J. L. 435-bp liver regulatory sequence in the liver fatty acid binding protein (L-FABP) gene is sufficient to modulate liver regional expression in transgenic zebrafish. *Dev. Dyn.* **227,** 347–356 (2003).
12. Loh, Y. H., Christoffels, A., Brenner, S., Hunziker, W. & Venkatesh, B. Extensive expansion of the claudin gene family in the teleost fish, *Fugu rubripes*. *Genome Res.* **14,** 1248–1257 (2004).
13. Wu, V. M., Schulte, J., Hirschi, A., Tepass, U. & Beitel, G. J. Sinuous is a *Drosophila* claudin required for septate junction organization and epithelial tube size control. *J. Cell Biol.* **164,** 313–323 (2004).
14. Behr, M., Riedel, D. & Schuh, R. The claudin-like megatrachea is essential in septate junctions for the epithelial barrier function in *Drosophila*. *Dev. Cell* **5,** 611–620 (2003).
15. Nitta, T. *et al.* Size-selective loosening of the blood–brain barrier in claudin-5-deficient mice. *J. Cell Biol.* **161,** 653–660 (2003).
16. Tsukita, S. & Furuse, M. Pores in the wall: claudins constitute tight junction strands containing aqueous pores. *J. Cell Biol.* **149,** 13–16 (2000).
17. Van Itallie, C. M. & Anderson, J. M. Claudins and epithelial paracellular transport. *Annu. Rev. Physiol.* **68,** 403–429 (2006).
18. Simon, D. B. *et al.* Paracellin-1, a renal tight junction protein required for paracellular $Mg^{2+}$ resorption. *Science* **285,** 103–106 (1999).
19. Hou, J., Paul, D. L. & Goodenough, D. A. Paracellin-1 and the modulation of ion selectivity of tight junctions. *J. Cell Sci.* **118,** 5109–5118 (2005).
20. Furuse, M., Furuse, K., Sasaki, H. & Tsukita, S. Conversion of zonulae occludentes from tight to leaky strand type by introducing claudin-2 into Madin–Darby canine kidney I cells. *J. Cell Biol.* **153,** 263–272 (2001).
21. Matter, K. & Balda, M. S. Functional analysis of tight junctions. *Methods* **30,** 228–234 (2003).
22. Van Itallie, C. M. & Anderson, J. M. The role of claudins in determining paracellular charge selectivity. *Proc. Am. Thorac Soc.* **1,** 38–41 (2004).
23. Gekle, M., Wunsch, S., Oberleithner, H. & Silbernagl, S. Characterization of two MDCK-cell subtypes as a model system to study principal cell and intercalated cell properties. *Pflügers Arch.* **428,** 157–162 (1994).
24. Grantham, J. J., Ye, M., Gattone, V. H. & Sullivan, L. P. *In vitro* fluid secretion by epithelium from polycystic kidneys. *J. Clin. Invest.* **95,** 195–202 (1995).
25. Li, H., Findlay, I. A. & Sheppard, D. N. The relationship between cell proliferation, $Cl^-$ secretion, and renal cyst growth: a study using CFTR inhibitors. *Kidney Int.* **66,** 1926–1938 (2004).
26. Kubota, K. *et al.* $Ca^{2+}$-independent cell-adhesion activity of claudins, a family of integral membrane proteins localized at tight junctions. *Curr. Biol.* **9,** 1035–1038 (1999).
27. Husain, N. *et al.* The agrin/perlecan-related protein eyes shut is essential for epithelial lumen formation in the *Drosophila* retina. *Dev. Cell* **11,** 483–493 (2006).
28. Tonning, A. *et al.* A transient luminal chitinous matrix is required to model epithelial tube diameter in the *Drosophila* trachea. *Dev. Cell* **9,** 423–430 (2005).
29. Devine, W. P. *et al.* Requirement for chitin biosynthesis in epithelial tube morphogenesis. *Proc. Natl Acad. Sci. USA* **102,** 17014–17019 (2005).
30. Lowery, L. A. & Sive, H. Initial formation of zebrafish brain ventricles occurs independently of circulation and requires the *nagie oko* and *snakehead/atp1a1a.1* gene products. *Development* **132,** 2057–2067 (2005).
31. Dong, P. D. *et al.* Fgf10 regulates hepatopancreatic ductal system patterning and differentiation. *Nature Genet.* **39,** 397–402 (2007).